

Noise-assisted transmission of spikes in Maeda-Makino artificial neuron arrays

Enrico Prati, Ernesto Giussani, Giorgio Ferrari & Tetsuya Asai

To cite this article: Enrico Prati, Ernesto Giussani, Giorgio Ferrari & Tetsuya Asai (2016): Noise-assisted transmission of spikes in Maeda-Makino artificial neuron arrays, International Journal of Parallel, Emergent and Distributed Systems, DOI: [10.1080/17445760.2016.1189914](https://doi.org/10.1080/17445760.2016.1189914)

To link to this article: <http://dx.doi.org/10.1080/17445760.2016.1189914>



Published online: 10 Jun 2016.



Submit your article to this journal [↗](#)



Article views: 7



View related articles [↗](#)



View Crossmark data [↗](#)

Noise-assisted transmission of spikes in Maeda–Makino artificial neuron arrays

Enrico Prati^a, Ernesto Giussani^{a,b}, Giorgio Ferrari^c and Tetsuya Asai^d

^aIstituto di Fotonica e Nanotecnologie, Consiglio Nazionale delle Ricerche, Milano, Italy; ^bDipartimento di Fisica, Università degli Studi di Milano, Milano, Italy; ^cDipartimento di Eletttronica, Informazione e Bioingegneria, Politecnico di Milano, Milano, Italy; ^dGraduate School of Information Science and Technology, Hokkaido University, Sapporo, Japan

ABSTRACT

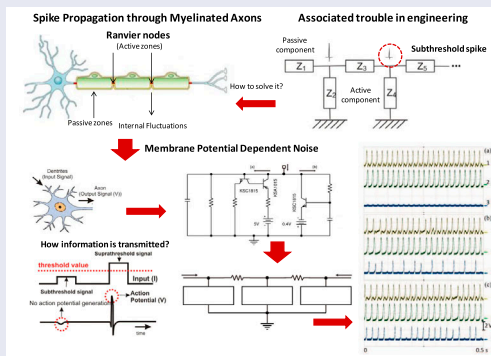
Experiment on artificial neurons are usually carried in ideal electronic environment aimed to minimise the disturbance generated by electronic noise. On the contrary, biological neurons are actively using the noise naturally present in their environment. Synaptic processes are noise-tolerant and in some cases noise-assisted. Enhancement of spike transmission assisted by noise has been proposed for arrays of artificial neurons, to emulate behaviour of biologically-plausible spike transmission among real neurons. We employ a biophysically meaningful hardware spiking neuron model reproducing bursting discharges of action potentials to experimentally realise noise-assisted spike transmission. The circuit consists of an array of artificial neurons equipped with Gaussian noise sources capable to deliver the noise current at the inter-neuron nodes. We simulate and experimentally demonstrate the enhancement of spike transmission by tuning Gaussian noise added at the input node of hardware neurons. The circuit provides experimental demonstration of noise-assisted enhancement of spike transmission along an array of weakly coupled neurons.

ARTICLE HISTORY

Received 10 May 2016
Accepted 11 May 2016

KEYWORDS

Artificial neurons;
Maeda–Makino neuron;
biologically inspired neural
networks; noise-assisted
spike transmission



Experimental demonstration of noise-assisted spike transmission in an electronic circuit representing an array of artificial membranes/neurons. In a chain of 3 neurons coupled by inhomogeneous resistors, spikes were not transmitted over the chain (a) if no noise were give, whereas spikes were travelled over the chain when the amount of the noise was increased (b)(c).

1. Introduction

We report on the first ever experimental demonstration of noise-assisted spiking activity in a circuit representing artificial neurons. Many biological systems can complete more efficiently some tasks with the assistance of noise [2,10,20]. With the aim of creating neural-processing microcircuits [18] based on biologically meaningful mechanisms including physically relevant aspects, we introduce electrical noise in spike transmission, generally present in the brain environment [3], and naturally present in atomic scale devices [9,14,15] suitable to replace 180 nm node CMOS currently employed in neuromorphic architectures [6]. Information transmission with noise assistance has already been studied in bistable [7,21] and electrical systems [17]. Gonzalez-Carabarin et al. [5] already discussed the impact of noise on spike transmission in an array of FitzHugh–Nagumo artificial neurons theoretically. There, noise applied to the membrane node is considered, to investigate how noise enhances the performance of spike transmission in serially connected electrical circuits receiving subthreshold inputs.

Here, we consider a different kind of neuron, namely the Maeda–Makino [8] to ensure high biological significance [12], and we simulate the arrays made of such neurons arranged as 1-dimensional chains interconnected by resistances [5]. Next, we experimentally explore the spike transmission between the neurons connected by resistors, and define the threshold resistance for the transmission and suppression. We then restore spike transmission by applying a Gaussian noise at the nodes between two neighboring neurons. In Section 2, the Methods are described, including neuron circuit, voltage to current conversion adopted scheme based on the Howland current pump circuit [4], and simulations. Section 3 describes the experiment of the use of Gaussian noise to restore spiking activity of a chain of Maeda–Makino hardware neurons (HNs) suppressed by synaptic high resistance. Section 4 is devoted to the summary.

2. Methods

We introduce the basic circuit acting as artificial neurons, the circuit representing an array of N artificial neurons connected in series by the simplest synapse element (a resistor), and the SPICE simulations showing the existence of a threshold resistance above which spike transmission is forbidden.

2.1. Scheme of single neuron

In the following, we briefly summarise the key features of the biologically-plausible artificial neuron employed in our circuit. We adopted the Maeda–Makino pulse-type HN model [8], analogue to four branches electrical equivalent circuit of Hodgkin–Huxley (HH) equation (Figure 1). C_a and R_d represent the membrane capacitance and the leakage resistance, respectively. The branches (a) and (b) emulate the voltage dependent inward sodium and the delayed outward potassium ionic channels, respectively. The branch (a) includes npn-type bipolar transistor KSC1815, and pnp-type bipolar transistor KSA1015, while the branch (b) the npn-type only. The HN is fed by current I_i which varies according to the experiment, while the potential V_i of the top nodes represents the membrane potential. One of a typical experimental result, the tonic (regular or spontaneous) spiking of a single neuron (V_i vs. time), is shown in Figure 2.

2.2. Scheme of neurons array

Here, we describe the circuit of the array of artificial neurons and the use of Howland current pump circuits to inject noise current at the membrane nodes. The network circuit consists of an array of N HNs. An array with $N = 3$ is shown in Figure 3, where three HNs are connected in series via resistances R_1 and R_2 between the HN_1 with HN_2 , and HN_2 with HN_3 , respectively. In our experiments, the input dc current is given to the HN_1 . In agreement with simulations (see next subparagraph), we experimentally confirmed that the spikes generated by the HN_i excite spikes in HN_{i+1} when the resistance R_i remains below a threshold resistance around 30 k Ω . We connected HN_1 with HN_2 through a resistance

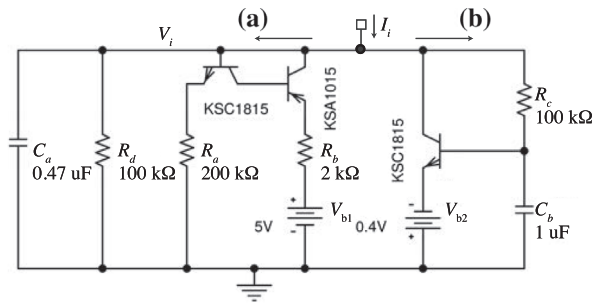


Figure 1. Maeda–Makino bursting HN basic model. The branches (a) and (b) correspond to the inward and the slow outward ionic channels, respectively. A more sophisticated version includes fast outward channel [8], not included in our experiment. C_d and R_d represent the membrane capacitance and the leakage resistance, respectively.

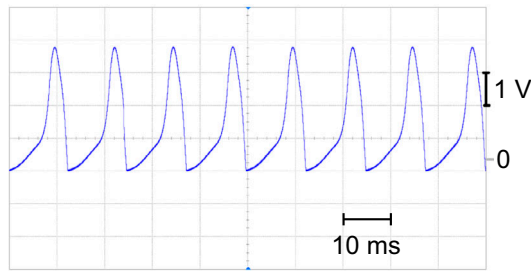


Figure 2. Experimental measurement of the tonic spiking of the basic Maeda–Makino HN. The circuit provides a robust and stable artificial neuron capable to reproduce biologically meaningful internal response, similar to current dynamics of ion channels. The HN is fed by the external current $I_i = 0.142$ mA. The vertical axis represents the membrane potential V_i .

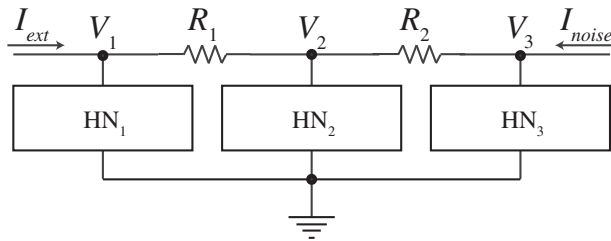


Figure 3. Diagram of the array of three HNs in series exploited for the experiment. The resistance R_1 is set sufficiently small to grant spike transmission, while R_2 stops the spikes unless some sufficiently large noise current I_{noise} is added at V_3 node.

$R_1 = 18$ kΩ, while $R_2 = 39$ kΩ. The current I_{ext} and I_{noise} injected in the first HN_1 and in the last HN_3 , respectively, were controlled with an external voltage generator via the voltage-to-current converter (Figure 4(b)).

The configuration employed for the experiment with noise is shown in Figure 4(a). By exploiting the basic circuit, a small resistance is employed between HN_1 and HN_2 to ensure spike transmission, while a large resistance among HN_2 and HN_3 is used to stop the spike transmission in standard condition, in order to explore the use of noise to restore spiking transmission even if the resistance would prevent it. Two Howland current pump circuits shown in Figure 4(b) are employed to inject current by using a dc voltage generator and a noise voltage generator, for spiking activity and for restoring spike transmission respectively.

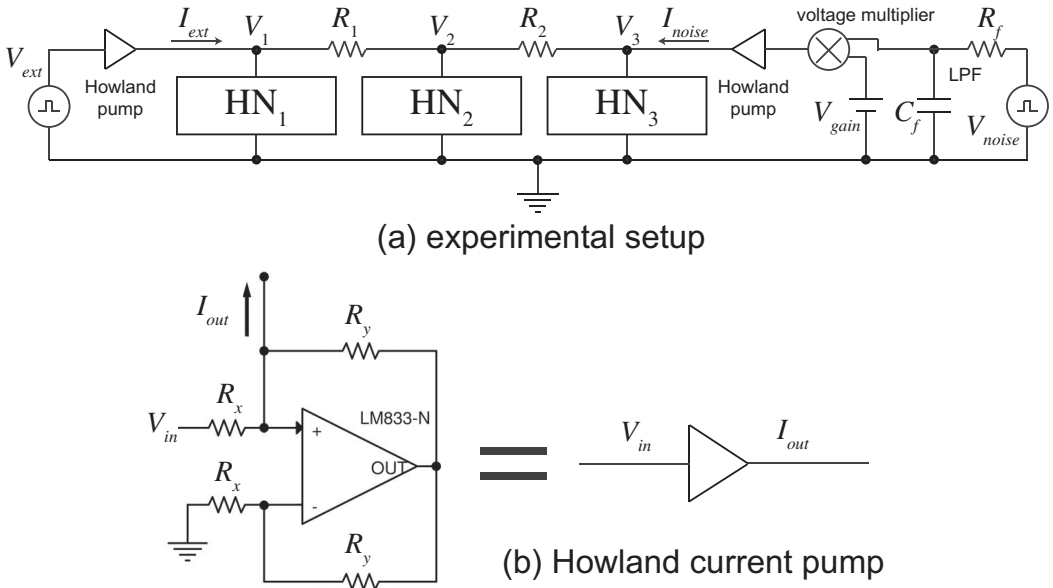


Figure 4. Array of HNs: (a) experimental setup and (b) Howland current pump circuit. The voltage noise is converted in a bipolar current noise using the Howland current pump circuit. The circuit has also been employed to implement the constant current source I_{ext} . Here $R_x = R_y = 910 \, \Omega$ with a conversion factor of $1.1 \, \text{mA/V}$.

2.3. SPICE simulations

In order to explore the effect of the resistance connecting each neuron to the next one, we first introduce the *threshold resistance* R_{th} of an array of N neurons. We define R_{th} as the minimum resistance capable to suppress at its end the spiking transmission along a 1-dimensional chain of N spiking neurons, connected two by $N - 1$ resistances of value R_{th} and whose first element is excited by DC current I_{ext} . To determine the threshold resistance for suppressing the fundamental spike transmission, an array of HNs without giving I_{noise} has extensively been simulated using a SPICE simulator (ngspice). The resistance connecting neighboring neurons was changed from 1 to 100 k Ω , and all the resistances connecting the neurons set at the same value. Figure 5 shows simulated threshold resistance vs input current I_{ext} when $N = 3$. The results show that the threshold resistance decreases when the input current is raised.

3. Experiments

We introduce the experimental setup employed to introduce noise current at the membrane nodes, we discuss the determination of the threshold resistance when noise is not applied, and we exploit noise solicitation to restore synaptic transmission along the array when sufficiently large synaptic resistance would stop spike transmission.

3.1. Experimental setup

In the following experiment, we first constructed a prototype of a neuron array ($N = 3$), shown in Figure 4(a), following the scheme of Figure 3 described in previous section. The tunable noise sources are implemented starting from a dual-channel voltage function arbitrary noise generator (Agilent 81150A). The wide bandwidth voltage noise is low-pass filtered (5 kHz) by C_f and R_f , and further amplified by a factor 20 ($V_{gain} = 20 \, \text{V}$, a standard voltage multiplier consisting of THS3001) to obtain the required power spectral density. The voltage noise is converted in a bipolar current noise using

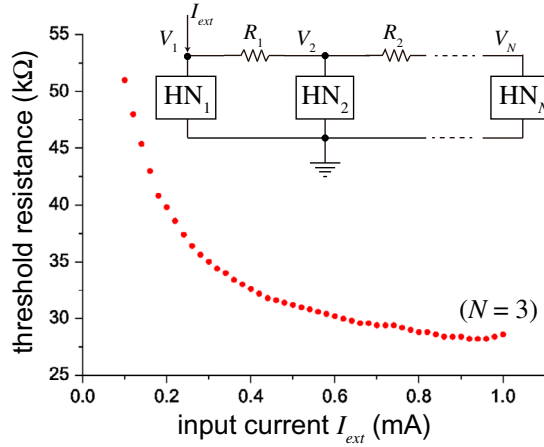


Figure 5. Threshold resistance for an array of three basic Maeda–Makino HNs as determined by ngspice simulations. The threshold resistance of an array of neurons solicited by an input continuous current I_{ext} consists of the minimum resistance capable to suppress the spiking transmission along the chain spiking neurons (see text). Threshold resistance decreases when the input current is raised.

the Howland current pump circuit shown in Figure 4(b). The feedback grants the same current in the R_y resistors and a current $V_{in}/(2R_x)$ in the R_x resistors. The Kirchoff current balance law at the input terminals of the operational amplifier sets the output current at $I_{out} = V_{in}/R_x$. The output resistance of the current pump is mainly limited by the tolerance of the resistors R_x and R_y , here chosen to obtain an output resistance greater than 100 kΩ. The same circuit has been used to implement the constant current source I_{ext} . Up to four artificial neurons are simultaneously monitored using a four-channel oscilloscope (Agilent DSO9254A).

3.2. Synaptic transmission: threshold resistance

In accordance with the simulations, the spike transmission between neighboring HNs is suppressed when the resistance is greater than threshold resistance evaluated in Figure 5. The threshold resistance is function of the intensity of the input current of the presynaptic HN previously referred as I_{ext} .

In Figure 6, the effect of the resistance R_1 between two consecutive hardware neurons HN_1 and HN_2 is shown. The tonic spiking of the HN_1 (blue), generated by a input $I_{ext} = 0.142$ mA, excites the HN_2 (orange) when they are connected through a sufficiently small resistance $R_1 = 18$ kΩ (Figure 6(a)). By increasing the R_1 at the threshold value, here around $R_1 = 39$ kΩ in Figure 6(b), the excitation in HN_2 does not occur.

3.3. ISI statistics

The characterisation of the impact of the noise on the spiking activity statistics of an individual neuron has been carried and compared to simulations. In the experiment, a single neuron ($N = 1$) is solicited by the noise input current provided by the voltage function generator. The experimental data consisting in the time intervals among consecutive spikes are represented as ISI distribution and reported in Figure 7. In order to fit experimental data, the Gaussian noise input of the simulation is 1 KHz cut-off, with 100 μA variance. The result consists of the broadening of the peak in the proximity of the natural tonic spiking frequency of the neuron, which is roughly 60 Hz at 100 μA (here $R_x = R_y = 10$ kΩ). The peak exhibits an exponentially decreasing right tail. The result is similar to that reported in [19] for Gaussian noise.

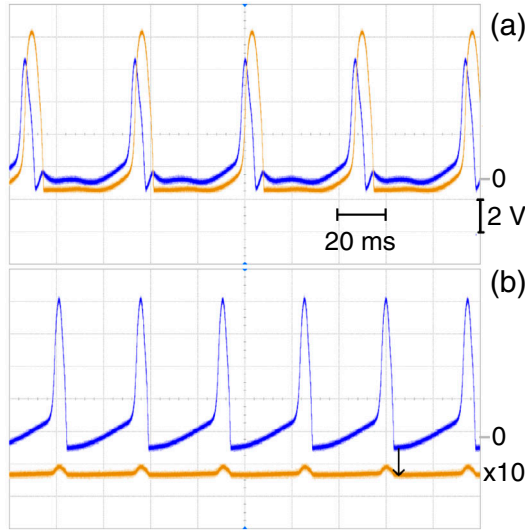


Figure 6. Role of the resistance R_1 for controlling excitation between neighboring HNs. The tonic spiking of the HN_1 (blue) excites the HN_2 (orange) when they are connected through a resistance $R_1 = 18 \text{ k}\Omega$ (a) at $I_{\text{ext}} = 0.142 \text{ mA}$. When the resistance is raised at the threshold resistance, here $R_1 = 39 \text{ k}\Omega$, the excitation does not occur (b).

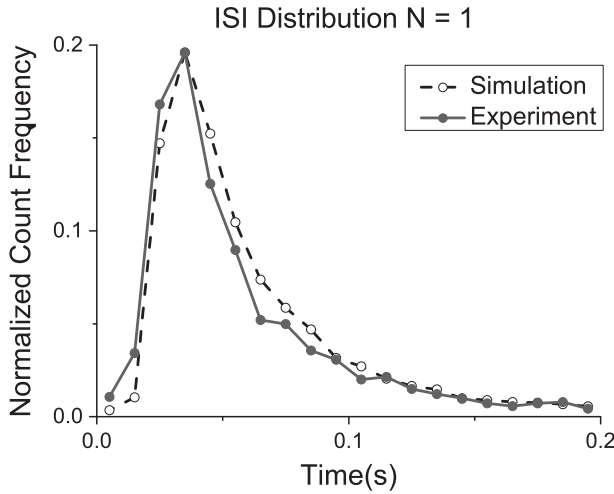


Figure 7. Interspike interval (ISI) distribution for a single neuron. The solid line (black points) represent the experimental data extracted for a $I_{\text{ext}} = 100 \mu\text{A}$, for $R_x = R_y = 100 \Omega$. The simulated noise is obtained by employing a Gaussian noise cut-off by a 1 KHz band with $100 \mu\text{A}$ variance.

3.4. Noise-assisted synaptic transmission

The experiment consists in the preparation of an array shown in Figure 4(a), namely, the direct excitation across a small resistance between HN_1 and HN_2 , and a large resistance among HN_2 and HN_3 . By applying the only I_{ext} , the spike transmission through the series of nodes is interrupted by resistances exceeding the threshold resistance. Our experiment consist in the recovery of spike transmission by adding a current noise source I_{noise} in correspondence of the HN_2 – HN_3 connection, as predicted in [5] and by the specific simulation carried for the circuit described above. In the noise-assisted spike transmission experiment, $R_1 = 18 \text{ k}\Omega$ and $R_2 = 39 \text{ k}\Omega$. The HN_1 is fed by a DC current of $I_{\text{ext}} = 0.22 \text{ mA}$

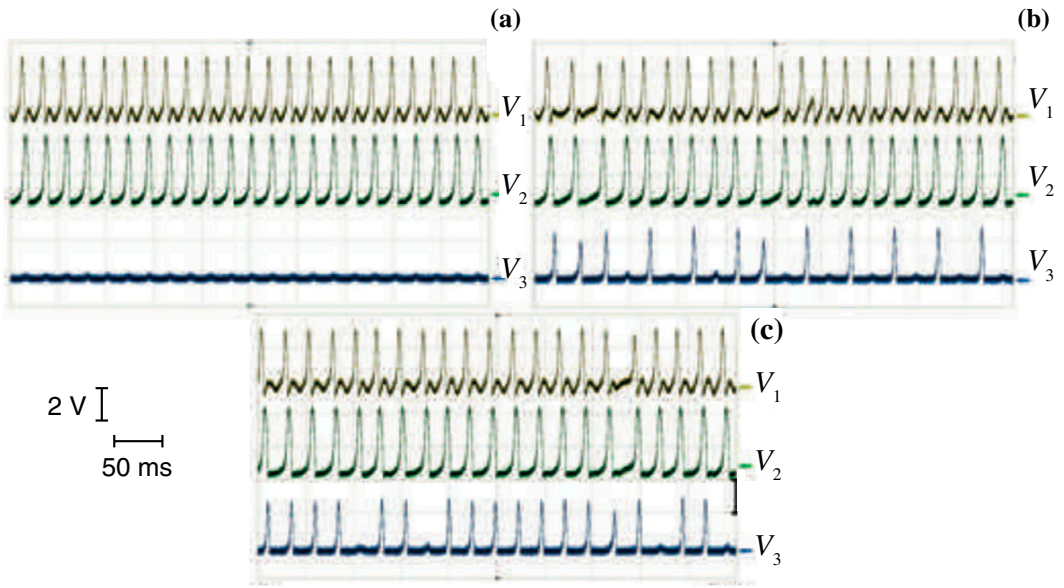


Figure 8. Noise-assisted spike transmission experiment. The Maeda–Makino nodes HN_1 and HN_2 are connected via a resistance $R_1 = 18 \text{ k}\Omega$, sufficiently small to let the HN_2 able to be excited by the first. According to simulations, at the nominal current $I_{\text{ext}} = 220 \text{ }\mu\text{A}$ employed in the experiment, the transmission is suppressed when the resistance overcomes the threshold of $37 \text{ k}\Omega$. Therefore, the HN_2 and the HN_3 are connected with a larger resistance, $R_2 = 39 \text{ k}\Omega$ which suppresses the spike transmission towards HN_3 in dc condition when only the HN_1 is fed by a current I_{ext} (a) When the noise at the HN_2 is either not present or insufficient (here $I_{\text{noise}} = 25 \text{ }\mu\text{A}$, i.e. the 11% of I_{ext}), the voltage spikes of HN_1 (V_1) are replicated by HN_2 (V_2), but not by HN_3 (V_3). The experiment consists in the addition of a current Gaussian noise at the second node with increasingly high variance I_{noise} , in order to restore spike transmission after HN_3 -blue line of (b) for $I_{\text{noise}} = 75 \text{ }\mu\text{A}$ (34% of I_{ext}), up to almost complete recovery when spikes pulsed by HN_1 (V_1) are largely replicated by HN_3 -blue line of (c) for $I_{\text{noise}} = 98 \text{ }\mu\text{A}$ (44% of I_{ext}).

which results from the conversion of a 200 mV control voltage reference through $R_f = 910 \text{ }\Omega$. The second node is fed by both the spiking current pulses generated by the HN_1 , and the Gaussian noise current I_{noise} .

In order to determine the value of the noise current imposed to HN_2 generated by the voltage function generator Agilent 81150A in Max Bandwidth Amplifier mode, the Gaussian noise with average equal to 0 has a bandwidth of 120 MHz (crest factor $V_{\text{peak}}/V_{\text{rms}} = 7$ was set). As the voltage signal is inescapably subject in our setup to a 5 kHz pass-band filter with $R_f = 910 \text{ }\Omega$, $C_f = 68 \text{ nF}$, and next amplified of a factor of 20, V_{noise} at HN_2 is $20 \times V_{\text{rms}} \times (5 \text{ kHz} / 120 \text{ MHz})^{1/2} \sim 0.13 V_{\text{rms}}$. Figure 8(a) shows the starting condition when the system is not perturbed by noise current at the second node. V_1 , V_2 and V_3 represent the membrane voltage of HN_1 , HN_2 and HN_3 , respectively. Such output remains unchanged for small variance of the noise. When the variance is sufficiently high (such as $I_{\text{noise}} = V_{\text{noise}}/R_f = 75 \text{ }\mu\text{A}$ as in Figure 8(b)), part of the spikes are randomly generated by HN_3 .

When the current achieves the maximum value provided by the settings of the equipment, namely $I_{\text{noise}} = 98 \text{ }\mu\text{A}$ which is about 44% of I_{ext} , almost all the spikes of HN_1 (V_1) and transmitted to HN_2 (V_2) are replicated in HN_3 (V_3), as shown in Figure 8(c).

4. Conclusion

We reported on experimental demonstration of noise-assisted spike transmission in a system made of Maeda–Makino biologically meaningful neurons. Inspired by those biological systems which can efficiently carry some tasks with the assistance of noise, with the aim of creating nanoelectronic neuromorphic architectures based on biologically meaningful mechanisms including multiple physically relevant aspects [5], we introduced the contribution of electrical noise on spike transmission.

The presence of electric noise and the ability to control it in atomic scaled devices [9,11,13,16] makes viable the route of employing such features in neuromorphic devices and circuits [1] to be designed in nodes beyond currently used 180 nm CMOS node.

Acknowledgements

The authors thank Raffaella Burioni (Università degli Studi di Parma, Italy) for useful discussions.

Disclosure statement

No potential conflict of interest was reported by the authors.

Funding

This study was supported by a Grant-in-Aid for Scientific Research on Innovative Areas [25110015] from the Ministry of Education, Culture, Sports, Science and Technology (MEXT) of Japan.

References

- [1] T. Asai and F. Peper, Explorations in morphic architectures, in *Emerging Nanoelectronic Devices*, 1st ed., A. Chen, J. Hutchby, V. Zhirnov, and G. Bourianoff, eds., Wiley and Sons, New Jersey, 2015, Chapter 22, pp. 443–455.
- [2] J.W. Brascamp, R. Van Ee, A.J. Noest, R.H. Jacobs, and A.V. van den Berg, *The time course of binocular rivalry reveals a fundamental role of noise*, *J. Vis.* 6(11) (2006), pp. 1244–1256.
- [3] A.A. Faisal, L.P. Selen, and D.M. Wolpert, *Noise in the nervous system*, *Nat. Rev. Neurosci.* 9(4) (2008), pp. 292–303.
- [4] S. Franco, *Design with Operational Amplifiers and Analog Integrated Circuits*, 3rd ed., McGraw-Hill, New York, 2002, p. 66.
- [5] L. Gonzalez-Carabarin, T. Asai, and M. Motomura, *Impact of noise on spike transmission through serially-connected electrical FitzHugh–Nagumo circuits with subthreshold and suprathreshold interconductances*, *J. Sign. Proc.* 16(6) (2012), pp. 503–509.
- [6] G. Indiveri, B. Linares-Barranco, T.J. Hamilton, A.V. Schaik, R. Etienne-Cummings, T. Delbruck, S. Liu, P. Dudek, P. Häfliger, S. Renaud, J. Schemmel, G. Cauwenberghs, J. Arthur, K. Hynna, F. Folowosele, S. Saighi, T. Serrano-Gotarredona, J. Wijekoon, Y. Wang, and K. Boahen, *Neuromorphic silicon neuron circuits*, *Front. Neurosci.* 5(73) (2011), pp. 1–23.
- [7] J.F. Linder, S. Chandramouli, A.R. Bulsara, M. Locher, and W.L. Ditto, *Noise enhanced propagation*, *Phys. Rev. Lett.* 81(23) (1998), pp. 5048–5051.
- [8] Y. Maeda and J. Makino, *A pulse-type hardware neuron model with beating, bursting excitation and plateau potential*, *BioSystems* 58 (2000), pp. 93–100.
- [9] G. Mazzeo, E. Prati, M. Belli, G. Leti, S. Cocco, M. Fanciulli, F. Guagliardo, and G. Ferrari, *Charge dynamics of a single donor coupled to a few-electron quantum dot in silicon*, *Appl. Phys. Lett.* 100 (2012), pp. 213107-1–213107-4.
- [10] D. Nozaki, D.J. Mar, P. Grigg, and J.J. Collins, *Effects of colored noise on stochastic resonance in sensory neurons*, *Phys. Rev. Lett.* 82(11) (1999), pp. 2402–2405.
- [11] E. Prati, *The finite quantum grand canonical ensemble and temperature from single-electron statistics for a mesoscopic device*, *J. Stat. Mech.* 2010 (2010), pp. P01003-1–P01003-9.
- [12] E. Prati, *Atomic scale nanoelectronics for quantum neuromorphic devices*, *Int. J. Nanotech.* (in press).
- [13] E. Prati, M. Belli, M. Fanciulli, and G. Ferrari, *Measuring the temperature of a mesoscopic electron system by means of single electron statistics*, *Appl. Phys. Lett.* 96 (2010), pp. 113109-1–113109-3.
- [14] E. Prati, M. De Michielis, M. Belli, S. Cocco, M. Fanciulli, D. Kotekar-Patil, M. Ruoff, D.P. Kern, D.A. Wharam, J. Verduijn, G.C. Tettamanzi, S. Rogge, B. Roche, R. Wacquez, X. Jehl, M. Vinet, and M. Sanquer, *Few electron limit of n-type metal oxide semiconductor single electron transistors*, *Nanotechnology* 23(21) (2012), pp. 215204-1–215204-5.
- [15] E. Prati and M. Fanciulli, *Manipulation of localized charge states in n-MOSFETs with microwave irradiation*, *Phys. Lett. A* 372(17) (2008), pp. 3102–3104.
- [16] E. Prati, M. Fanciulli, A. Calderoni, G. Ferrari, and M. Sampietro, *Microwave irradiation effects on random telegraph signal in a MOSFET*, *Phys. Lett. A* 370(5–6) (2007), pp. 491–493.
- [17] A.C.H. Rowe and P. Etchegoin, *Experimental observation of stochastic resonance in a linear electronic array*, *Phys. Rev. E* 64 (2001), pp. 031106-1–031106-4.
- [18] G. Silberberg, A. Gupta, and H. Markram, *Stereotypy in neocortical microcircuits*, *Trends Neurosci.* 25(5) (2002), pp. 227–230.

- [19] C. Sobie, A. Babul, and R. De Sousa, *Neuron dynamics in the presence of $1/f$ noise*, Phys. Rev. E 83(5) (2011), pp. 051912-1–051912-6.
- [20] P.N. Steinmetz, A. Manwani, C. Koch, M. London, and I. Segev, *Subthreshold voltage noise due to channel fluctuations in active neuronal membranes*, J. Comput. Neurosci. 9(2) (2000), pp. 133–148.
- [21] A.A. Zaikin, D. Topaj, and J. Garcia-Ojalvo, *Noise-enhanced propagation of bichromatic signals*, Fluct. Noise Lett. 2(1) (2002), pp. L47–L52.